

Project Phase 2

AER 1202 – Prof. Liu

Sam Weinberg (1005347634)

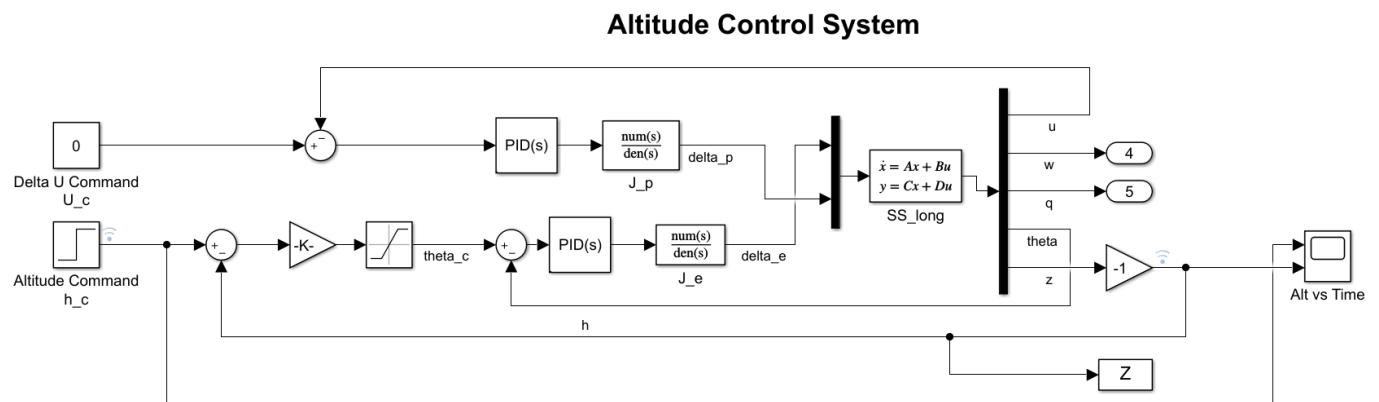
Navneet Gopinath (1005077319)

Phase 1 Overview

In phase 1, the linear dynamic model was developed, and the control system was designed based on the feedback from the outputs. To avoid excessive repetition, this report will omit the linear dynamics development and focus on the control system design, development of the nonlinear simulation, and comparison of the linear and nonlinear results. Please refer to phase 1 for the development of the linear dynamics.

1) Altitude Control System

The block diagram Simulink model for the altitude control is shown below. The diagram can be enlarged in the attached Simulink file.



The altitude command is a step input of Δh in metres, where the reference altitude is 40,000 ft as described in the question. As a result, the step input final value is 1524 m (5000 ft), which represents a climb from 40000 ft to 45000 ft as required. The throttle is used to maintain a velocity u of 235.9 m/s (Mach 0.8) during the ascent. Therefore, the Δu command is held at a constant zero to maintain the velocity, however this can be altered if another velocity is desired.

The altitude error is converted to a desired pitch angle through a gain and a limiter. The gain that produced reasonable results was reference from Etkins (pg. 280) to be 0.0002 (larger values were too responsive whereas smaller values produced long settling times). The limiter is used to maintain a desired pitch angle that is realistic and produces a smooth ascent. The maximum pitch angle was chosen to be 5 degrees; however this value can be altered as desired. The pitch angle error is propagated

through a PID control law system. Additionally, the elevator servo actuator block is used to simulate a realistic system with time constant 0.1. The overall control law is summarized as

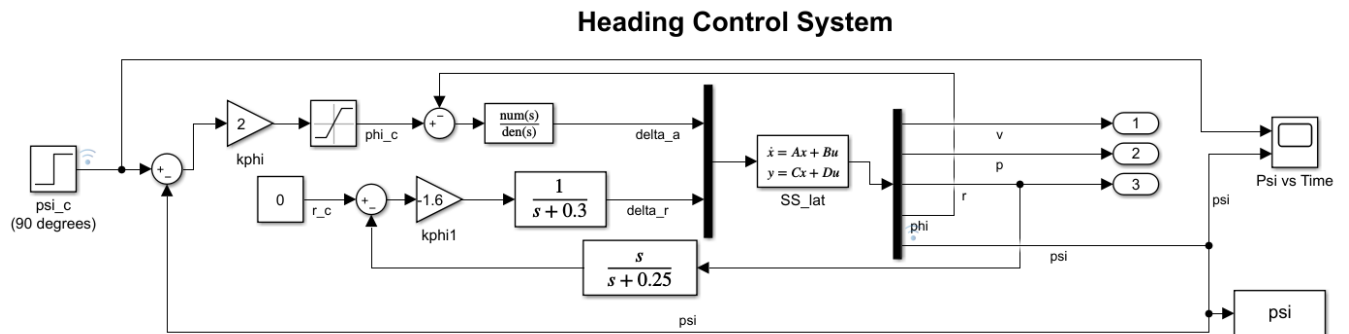
$$C(s) = \left(K_p + K_i \frac{1}{s} + K_d s \right) \left(\frac{1}{\tau_e s + 1} \right)$$

The PID controller constants were found using the PID tuner in Simulink. The PID tuner methodology can be found in the phase 1 report.

The resultant elevator input along with the throttle input, which was modelled in a similar manner (PID control and time delay), were input into the longitudinal state space model to obtain the state vector. Both the pitch angle and height difference were fed back to the desired commands to complete the closed loop system.

2) Heading Control System

The block diagram for the heading control system is displayed below. Again, an enlarged version is available in the Simulink file.



The proposed turning mechanism was to perform a steady banked turn using the ailerons to produce a desired roll angle. The yaw error was converted to a roll angle command using a somewhat arbitrarily selected gain of 2 (produced high response to minimize steady state error) and a limiter to maintain a maximum roll angle (25 degrees) that produced a smooth turn. The roll angle error was used to determine the required aileron deflection, which was controlled using a PID control law.

The PID coefficients were calculated using the PID tuner in Simulink. This was found to be more effective than Zeigler-Nichols tuning, and was easier to carry out with ongoing changes to the model. The PID tuning process is similar to that shown in the longitudinal model. The control law is summarized as

$$C(s) = K_p + K_i \frac{1}{s} + K_d s$$

The aileron and rudder deflections are input into the lateral state space model to calculate the state vector. The yaw and roll angles were used as feedback to the desired values.

3) Nonlinear Model

The nonlinear model is very similar to the linearized control system, except the nonlinear dynamics are substituted in place of the linearized state space models. Previously, the longitudinal and lateral dynamics were uncoupled, and the state space models were calculated separately. The two systems are now combined utilizing a coupled nonlinear dynamics subsystem with four inputs ($\delta_p, \delta_e, \delta_a, \delta_r$) and all twelve outputs. The nonlinear equations are rearranged and summarized, and the overall control design is demonstrated below.

$$\dot{u} = \frac{X}{m} - g \sin \theta - qw + rv$$

$$\dot{v} = \frac{Y}{m} - g \cos \theta \sin \phi - ru + pw$$

$$\dot{w} = \frac{Z}{m} - g \cos \theta \cos \phi - pv + qu$$

$$\dot{p} = \frac{1}{I_{xx}} (L + I_{zx} \dot{r} - qr(I_{zz} - I_{yy}) + I_{zx}pq)$$

$$\dot{q} = \frac{1}{I_{yy}} (M - rp(I_{xx} - I_{zz}) - I_{zx}(p^2 - r^2))$$

$$\dot{r} = \frac{1}{I_{zz}} (N + I_{zx} \dot{p} - pq(I_{yy} - I_{xx}) - I_{zx}qr)$$

$$\dot{\phi} = p + (q \sin \phi + r \cos \phi) \tan \theta$$

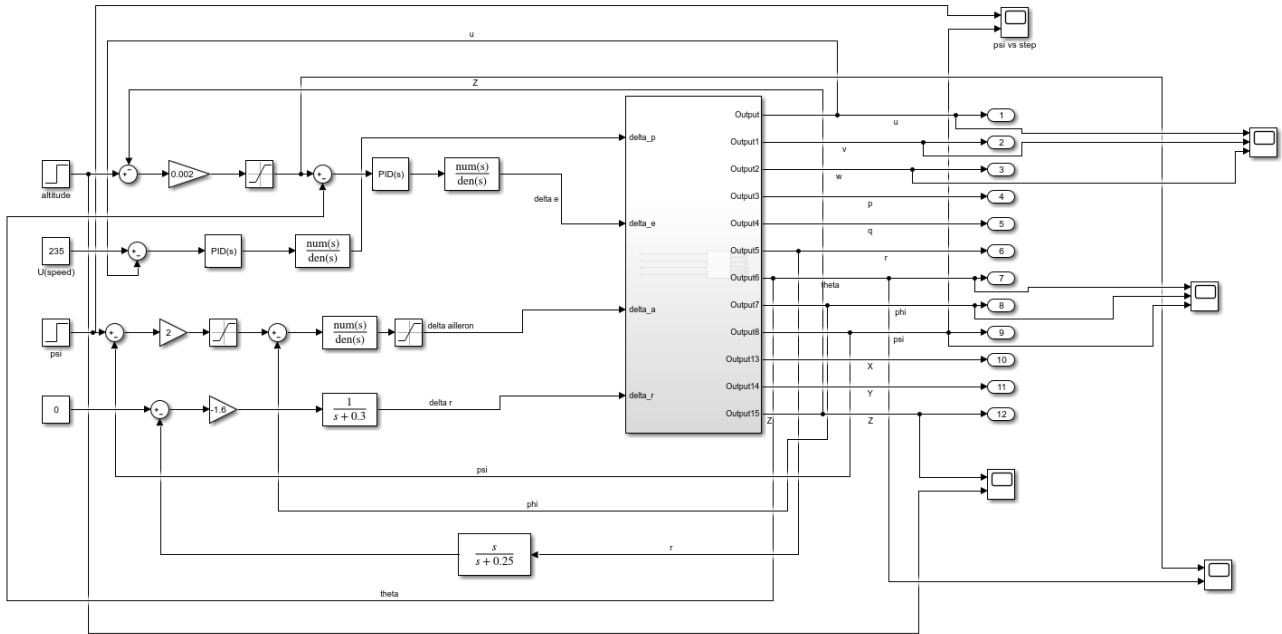
$$\dot{\theta} = q \cos \phi - r \sin \phi$$

$$\dot{\psi} = (q \sin \phi + r \cos \phi) \sec \theta$$

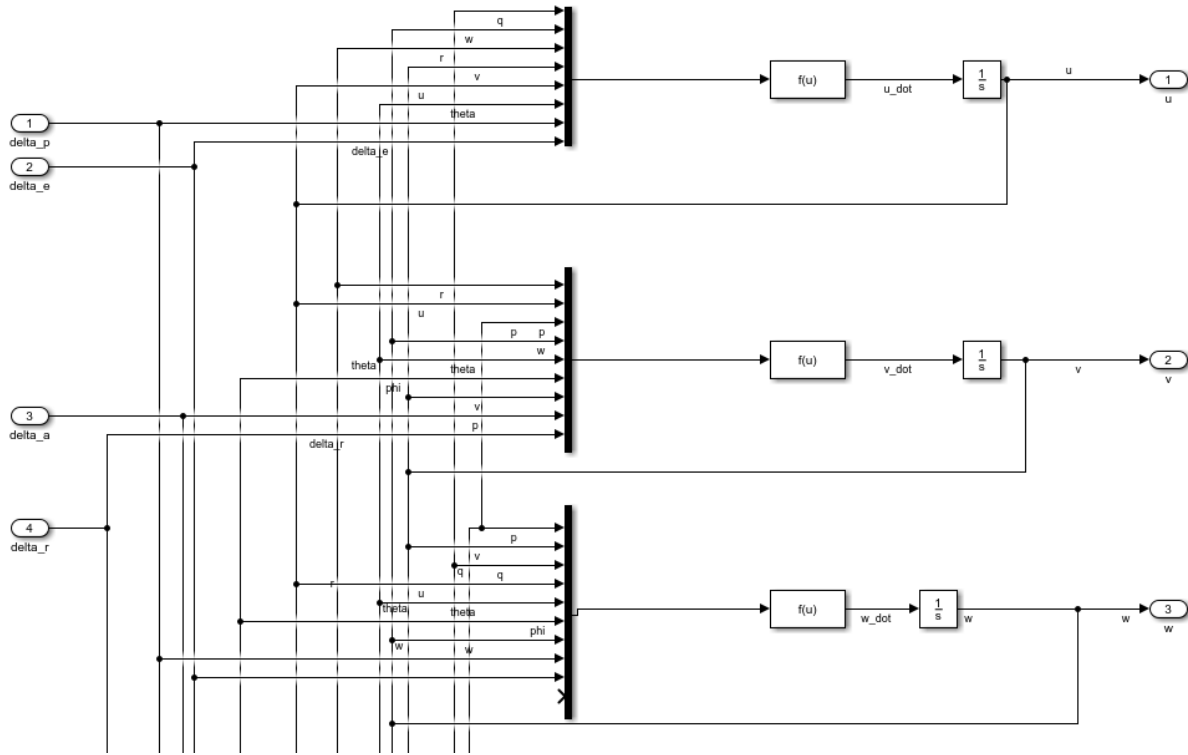
$$\dot{x}_E = u \cos \theta \cos \psi + v(\sin \phi \sin \theta \cos \psi - \cos \phi \sin \psi) + w(\cos \phi \sin \theta \cos \psi + \sin \phi \sin \psi)$$

$$\dot{y}_E = u \cos \theta \sin \psi + v(\sin \phi \sin \theta \sin \psi + \cos \phi \cos \psi) + w(\cos \phi \sin \theta \sin \psi - \sin \phi \cos \psi)$$

$$\dot{z} = -u \sin \theta + v \sin \phi \cos \theta + w \cos \phi \cos \theta$$



The Simulink file is attached to investigate this image as desired. The control and feedback loops are identical to the linear case, but the dynamics have been replaced. The nonlinear subsystem implements each of the above equations along with an integrator to calculate the parameters and their derivatives at each timestep. An excerpt of this subsystem is shown below for u , v , and w , and again the Simulink model is attached for further investigation.



The aerodynamic forces were calculated using the linearized model as before, where the total aerodynamic coefficients were calculated. The X direction aerodynamic coefficient calculation is shown as an example.

$$C_X = C_{x_0} + C_{x_u} u + C_{x_\alpha} w + C_{x_{\dot{\alpha}}} \dot{w} + C_{\delta_e} \delta_e + C_{\delta_p} \delta_p$$

A few control system modifications were required to implement the nonlinear system and achieve the desired results. Firstly, all the PID control laws were retuned using the PID tuner as described in the phase 1 report. The u velocity control input was set to a constant value of 235.9 m/s, whereas in the linearized model it was set to zero since this previously represent Δu . Additionally, the limiter used to control the desired pitch angle was adjusted to a maximum value of 10° . When the simulation was run using the same maximum value from the linear model (5°), the plane steadily loses altitude and is unable to climb to the desired altitude as shown below. This may be caused by an insufficient amount of lift to maintain this pitch angle.

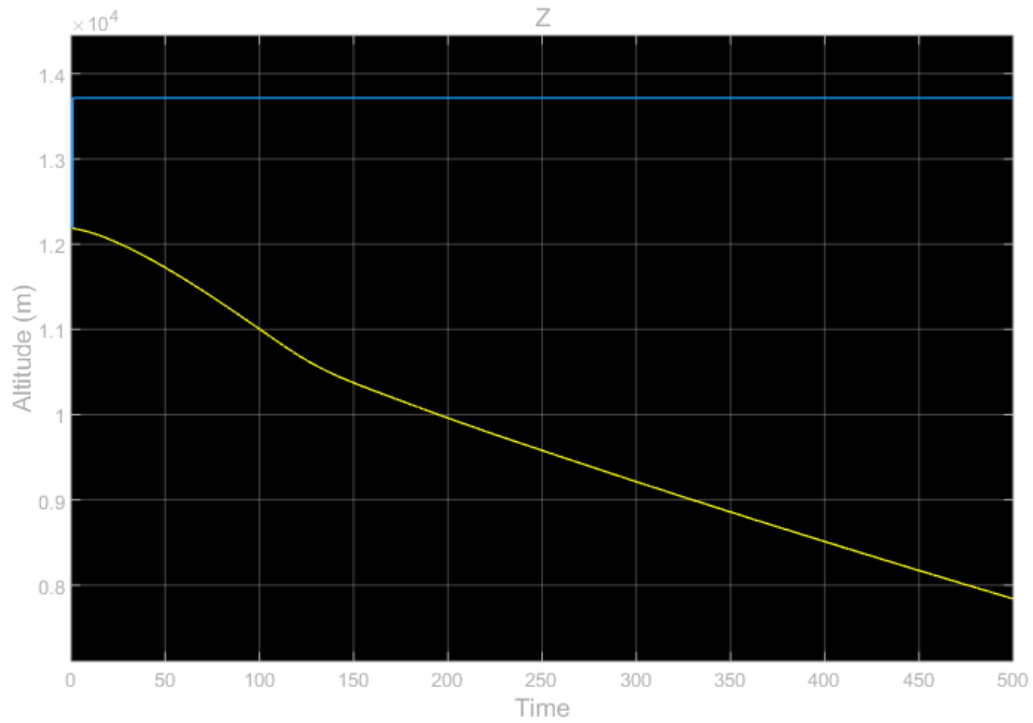


Figure 1: Altitude vs time for nonlinear system ($\theta = 5^\circ$).

4) Linear vs. Nonlinear Results

After adjusting the limiter to a maximum pitch angle of $\theta_{max} = 10^\circ$, the nonlinear simulation was observed to achieve reasonable results in agreeance with the linear model. The linear and nonlinear longitudinal system results are demonstrated below.

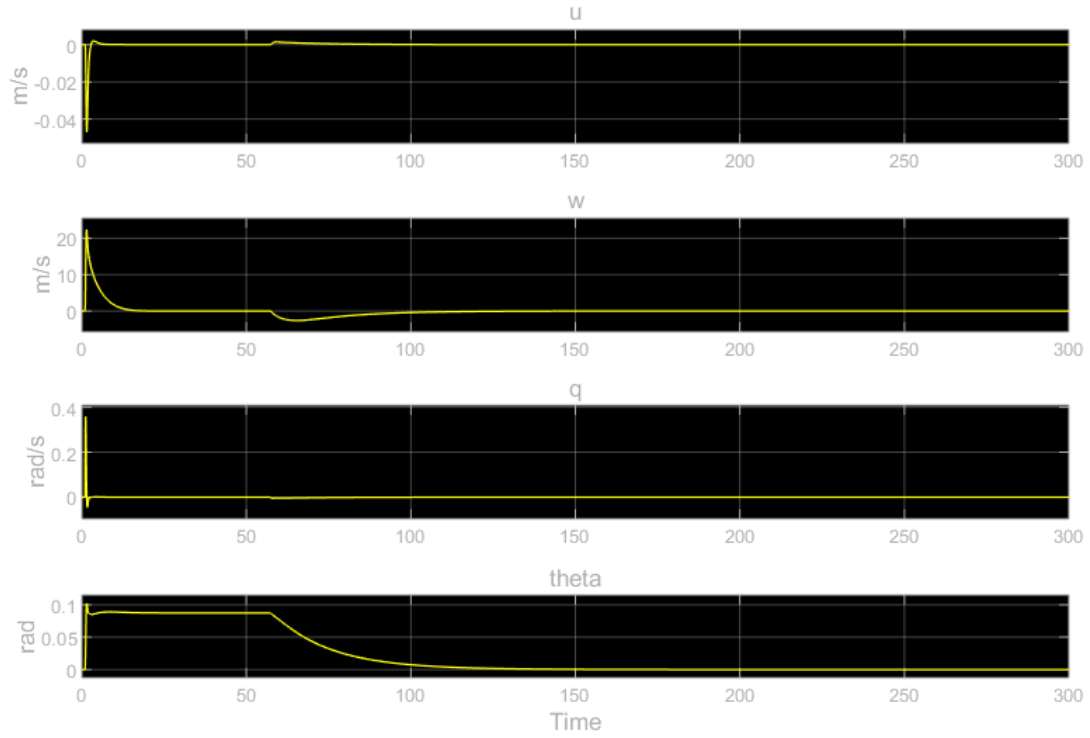


Figure 2 Linear - Longitudinal system response.

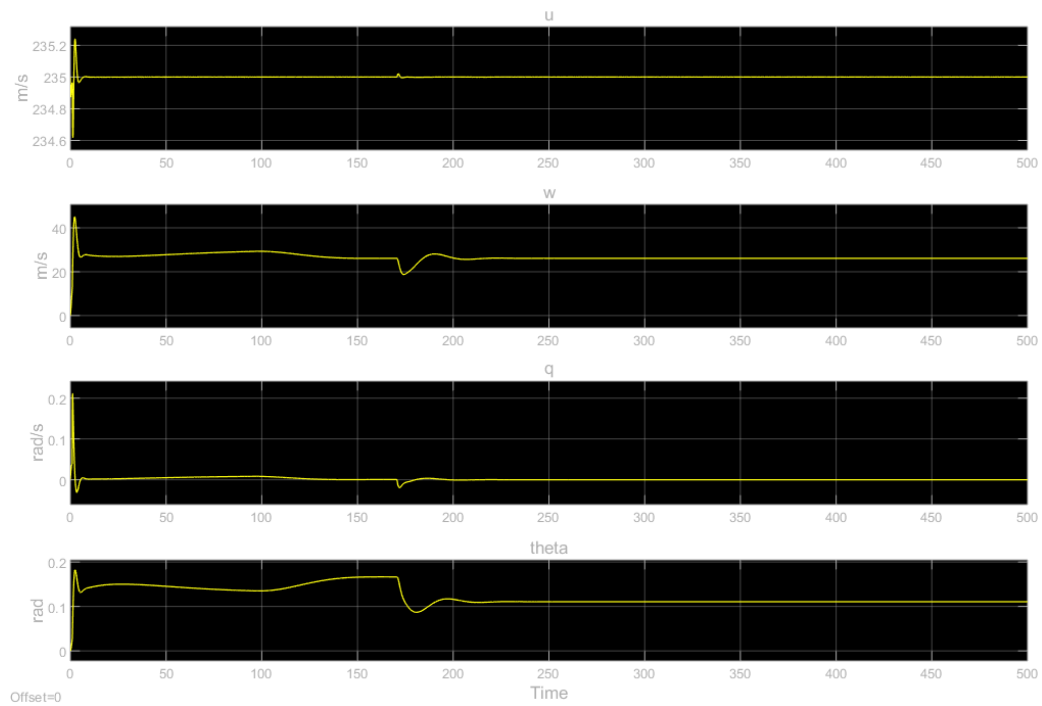


Figure 3: Nonlinear – Longitudinal system response.

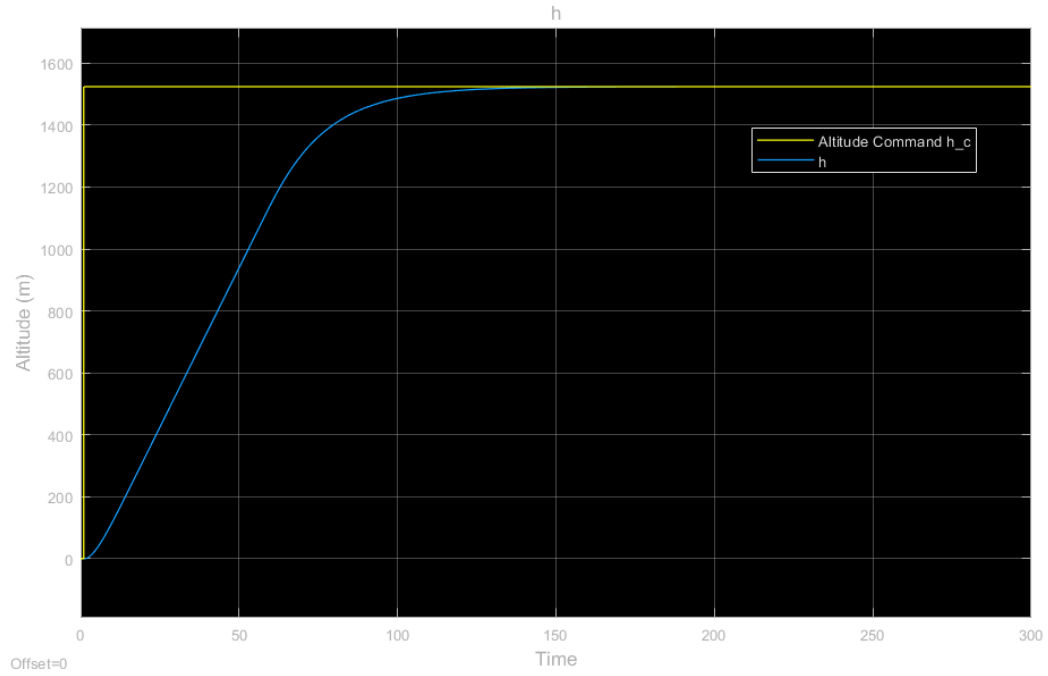


Figure 4: Linear model altitude response.

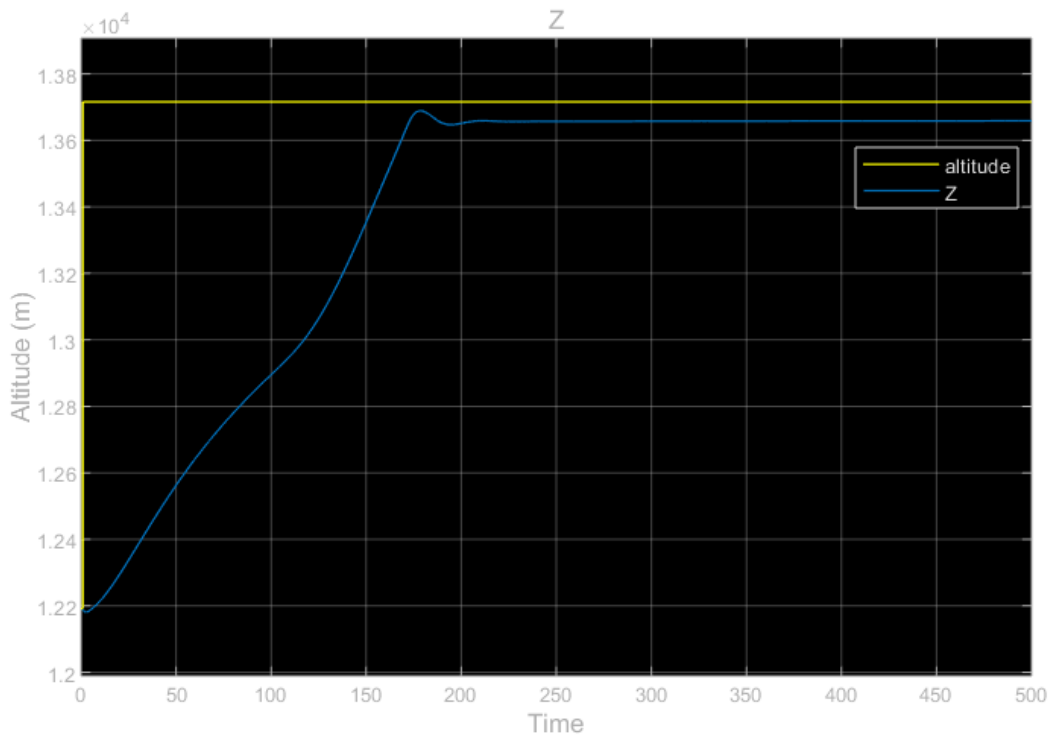


Figure 5: Nonlinear model altitude response.

The altitude response for the linear case has zero overshoot and a steady state error of less than 1%. For the nonlinear case the aircraft doesn't reach the desired altitude but settles with a steady state error of approximately 6.7%, just outside the design specifications. Additionally, the settling time is observed to be approximately double in the nonlinear response, which is unintuitive considering the increase in maximum pitch angle and may be caused by the coupling of the lateral system. The addition of the subsystem may also impact the simulation time due to its computational inefficiency in comparison to the built-in state space block.

Similarly, the nonlinear and linear results for the lateral system are displayed below. Again, the nonlinear simulation results were in good agreement.

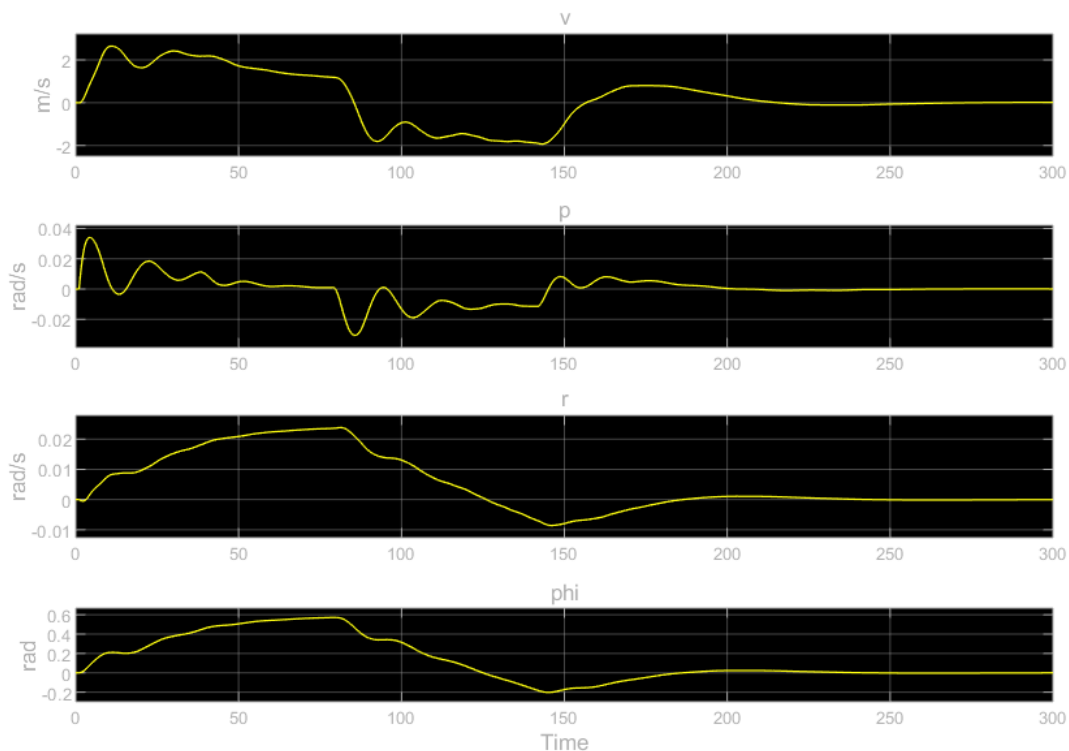


Figure 6 Linear - Lateral system response.

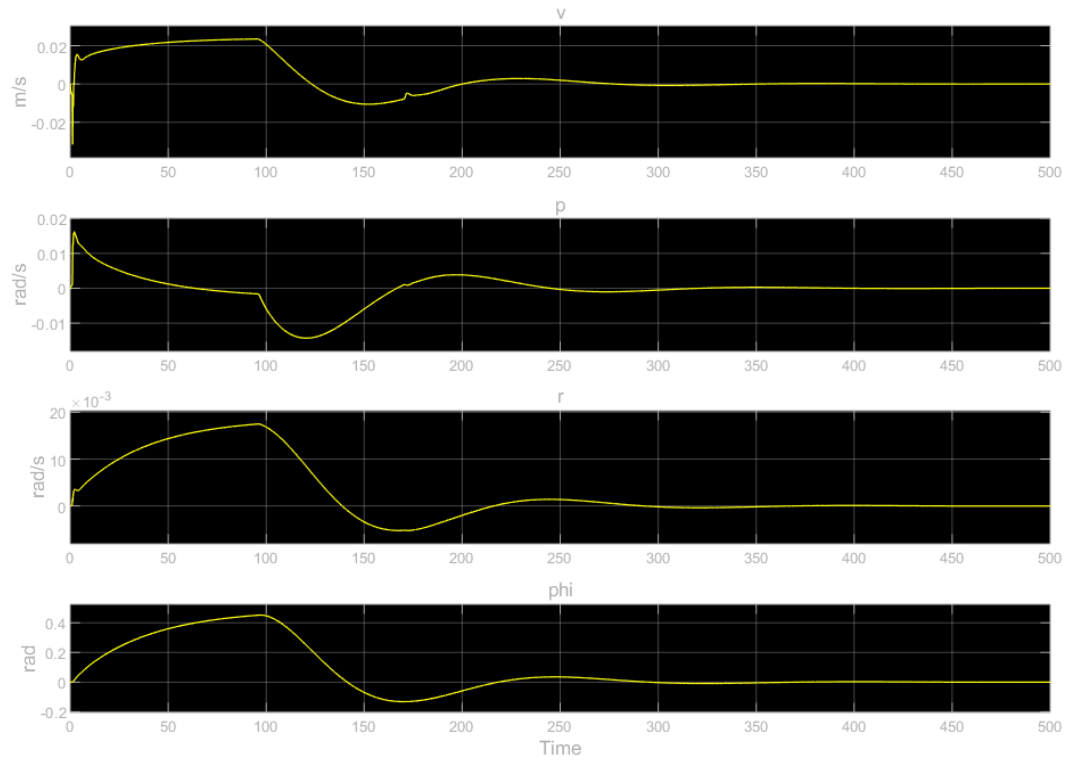


Figure 7: Nonlinear – Lateral system response.

Comparing the lateral system responses of the linear and the nonlinear, the overall response is similar except for the response of the nonlinear system being much smoother. The roll angle for the linear system is about 20% higher than the nonlinear system due to the limiter being set for a lower value in the nonlinear case.

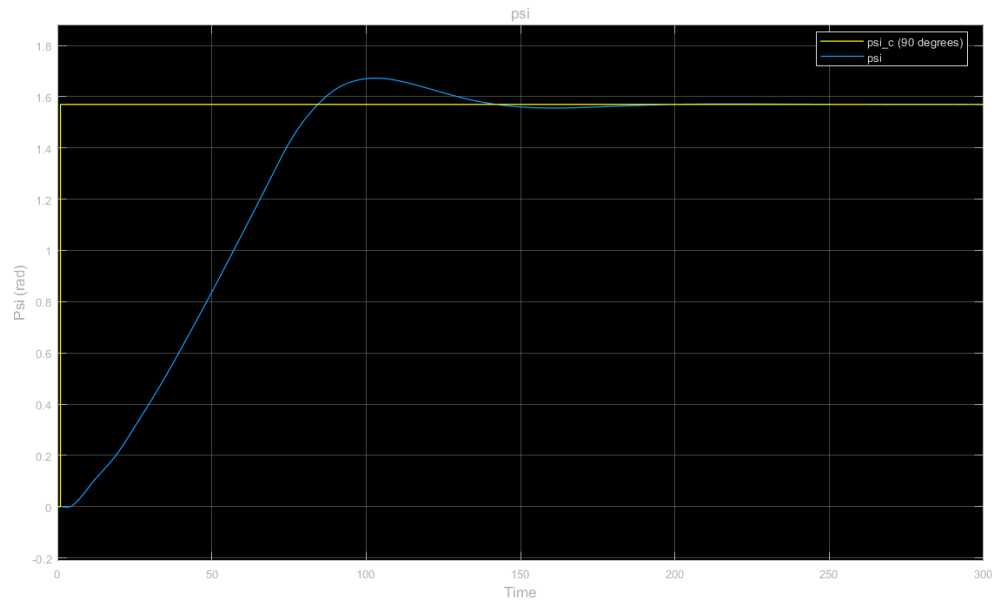


Figure 8: Linear model heading response.

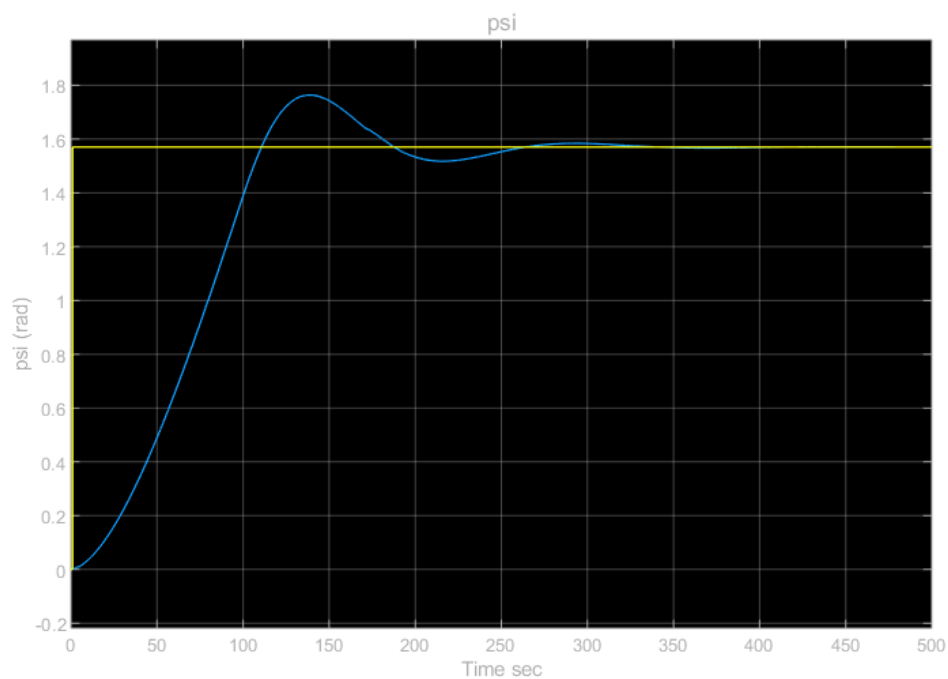


Figure 9: Nonlinear model heading response.

The heading control system shows a similar settling time difference (approximately factor of 2) between the linear and nonlinear response. This may further indicate that the subsystem has an impact on the settling time. While the linear results are well within the design specifications, the nonlinear system

produces approximately 12% overshoot with near zero steady state error. Although this doesn't satisfy the design criteria, the results are largely acceptable.

5) Conclusion

A heading and altitude control system was designed using the linearized equations of motion, and a Simulink model was developed. A nonlinear flight simulation was used to test the control system design and observe the differences between the linear and nonlinear dynamics. Overall, the nonlinear simulation produced reasonable results with the same dynamic behavior as the linear system. Discrepancies in settling time may be attributed to the addition of a subsystem producing additional time delays.